Responses to Reviewer 1

**This manuscript presents high-time-resolution measurements of aerosol chemical composition at MCOH and provides valuable molecular-level information on sulfate-containing organic compounds and highly oxidized organic aerosol over the northern Indian Ocean. The dataset is interesting and potentially useful for improving our understanding of aerosol characteristics in this region, especially given the limited availability of such measurements at this site. However, in its current form, the manuscript is more convincing in describing the observed aerosol composition than in demonstrating the proposed mechanisms controlling it. In particular, several key interpretations regarding long-range transport aging, aqueous/cloud processing, and the influence of Delhi or Indo-Gangetic Plain outflow are not yet sufficiently supported by the current analysis. I therefore think the a major reversion is needed before it can be considered for publication.**

We thank the reviewer for this overview and agree that a deeper analysis will improve our understanding of the results from this campaign. We have explored further analyses based on the reviewer's suggestions and have made substantial revision to the manuscript to reflect this. Specific points raised by the reviewer are addressed in more detail below.

**Major comments:**

1. **The manuscript separates the campaign into three periods associated with different air mass trajectories. However, this classification is not fully exploited in the subsequent analysis. Beyond showing bulk compositional similarities and differences in mass loading, the manuscript does not provide a sufficiently detailed analysis of molecular composition, source tracers of each period, or potential processing pathways. As a result, the period classification appears somewhat descriptive rather than mechanistically informative. If the authors aim to argue that aerosol processing during long-range transport governs the observed composition, a deeper comparison among these periods is needed.**

We thank the reviewer for this comment. We agree that the manuscript did not fully exploit the three transport periods beyond illustrating differences in aerosol mass loading and broad compositional characteristics.

To address this concern, we have expanded the discussion of the period-resolved observations and more explicitly compared the aerosol composition among the three transport regimes. We now highlight similarities and differences in bulk aerosol composition, the elemental composition of organic aerosol, and oxidation indicators derived from AMS measurements (O:C and $f_{44}$).

The revised analysis shows that, despite differences in air mass origin and total aerosol loading, the composition of organic aerosol remained remarkably consistent across the three periods. The AMS organic mass spectra and the elemental composition showed very little variation among the periods. These observations suggest that organic aerosol reaching MCOH had undergone substantial regional mixing and atmospheric processing before arrival, resulting in a relatively homogeneous aerosol composition despite differences in transport pathways.

We have also more explicitly investigated the changing ratio between sulfate and organic aerosol across the three periods. A concentration-weighted back-trajectory analysis indicates that sulfate aerosol concentrations are highest in air masses originating in the IGP, whereas organic aerosol appears to be much less dependent on transport history. This suggests that sulfate loading may serve as a tracer of IGP and anthropogenic influences at this site.

We have revised the Results and Discussion sections to emphasise this analysis and to clarify that the period classification is used primarily to assess the extent to which differences in transport history influence aerosol composition. The limited compositional differences observed among organic aerosol across the periods support the interpretation that regional-scale processes exert a stronger influence on aerosol composition at MCOH than the specific transport pathway sampled during individual periods. The changes in sulfate contribution suggest that this may provide a more robust understanding of IGP influence than organic aerosol composition.

**Changes to the manuscript**

The following text has been added to section 3.2:

The comparison of the three transport periods indicates that, although sulfate remained the dominant species in all cases, the fractional contribution of sulfate increased from one period to the next, while that of organic aerosol decreased. The contribution from nitrate remained low throughout. The chemical composition of organic aerosol was highly consistent across all three time periods. Characteristic parameters from all three time periods are shown in Table 1. Here it can be seen that the O:C ratio, H:C ratio, and the fractional contribution from *m/z* 44 ($f_{44}$), *m/z* 43 ($f_{43}$) and *m/z* 60 ($f_{60}$) showed very little variation, regardless of air mass origin. This compositional stability in organic aerosol across air masses arriving from different transport pathways suggests that the aerosol reaching MCOH had undergone extensive regional mixing and atmospheric processing before arrival. Consequently, differences in transport history were reflected more strongly in aerosol loading than in aerosol composition, indicating that regional-scale processing exerts a dominant influence on the chemical characteristics of the wintertime haze over the northern Indian Ocean.

A concentration-weighted back trajectory analysis of sulfate aerosol and organic aerosol suggests that, while both species are present in air masses regardless of transport history, the sulfate concentration is most prominent in air masses originating from the IGP, while organic aerosol did not show any preferential air mass origin (Fig. 3). This suggests that at this site, the fraction of sulfate observed in ambient aerosol may be useful as an indication of air masses that have been more strongly influenced by anthropogenic pollution in the IGP.

In addition, we have added a new table (Table 1) to summarise the key properties of aerosols observed during the three periods, and a new figure (Fig. 3) illustrating the concentration-weighted back-trajectory analysis for sulfate and organic aerosol.

2. **The manuscript argues that photochemical aging, aqueous/cloud processing, and sulfate-driven heterogeneous chemistry during long-range transport govern the aerosol composition at MCOH. However, the current evidence is still largely inferential, based mainly on back trajectories, compositional similarity across periods, high O:C, and the presence of highly oxidized compounds. These observations are consistent with atmospheric processing, but they do not by themselves uniquely demonstrate that these processes occurred during transport.**

We thank the reviewer for highlighting the important distinction between observations consistent with atmospheric processing and those that directly demonstrate specific processing mechanisms. We agree that the evidence presented in the original manuscript is primarily indirect and does not uniquely establish the occurrence of photochemical ageing, aqueous/cloud processing, or sulfate-driven heterogeneous chemistry during transport.

In response, we have revised the wording throughout the Discussion and Conclusions sections to more clearly distinguish between observation and interpretation. Rather than stating that these processes definitively govern aerosol composition at MCOH, we now state that the observations are consistent with, and support the likely importance of these processing pathways.

Our interpretation is based on several independent observations, including (i) the high degree of aerosol oxidation, (ii) the dominance of highly oxygenated compounds and dicarboxylic acids in the particle-phase organic aerosol, (iii) the prevalence of sulfate and sulfur-containing organic compounds commonly associated with sulfate-mediated chemistry, and (iv) the compositional similarity among air masses with different transport histories. Collectively, these observations support the interpretation that substantial atmospheric processing occurred before the aerosol arrived at MCOH.

However, we acknowledge that the available measurements do not provide direct process-level constraints sufficient to uniquely separate the relative contributions of photochemical, aqueous-phase and heterogeneous pathways. The revised manuscript now explicitly acknowledges this limitation and presents these mechanisms as plausible interpretations supported by the observed molecular composition, rather than as directly observed processes.

**Changes to the manuscript**

We have made some adjustments to the phrasing in section 3.2. Current: "These observations … indicate that the aerosol observed during this campaign was well-mixed and highly processed…"

New: These observations – both the relative stability of the aerosol chemical composition across source regions and the composition itself – are consistent with an aerosol population that has undergone extensive regional mixing and atmospheric processing during long range transport before arriving at MCOH. The similarity in composition across source regions, as evidenced by the similar aerosol composition across the three highlighted time periods, suggests that the regional-scale processing may exert a stronger influence on aerosol composition than variations in transport pathway.

In section 3.4, current: "Our observations are consistent with the previous suggestions that the majority of these SCOs…"

New: Our observations are consistent with previous suggestions that the majority of these SCOs are formed when biogenic VOCs – particularly isoprene – interact with inorganic sulfate aerosol during transport (Stone et al., 2012). However, the available measurements do not uniquely constrain the formation pathway or the identity of the precursors of the observed SCOs.

3. **The manuscript attributes the high abundance of oxalic acid and other dicarboxylic acids to cloud or aqueous-phase processing, which is plausible. However, the evidence presented here is still indirect. If the authors want to retain this as a central mechanistic conclusion, it would help to include additional analysis linking these species to meteorological or transport indicators relevant to aqueous processing, or at least to more clearly acknowledge that the conclusion is based on molecular interpretation rather than a direct process constraint.**

We agree that the attribution of oxalic acid and other dicarboxylic acids to aqueous-phase and cloud processing is based primarily on molecular evidence and interpretations informed by previous studies, rather than on direct observation of these processes.

In response, we have revised the manuscript to more clearly distinguish between observation and interpretation. The revised text now states that the high abundance of oxalic acid and other dicarboxylic acids is consistent with aqueous-phase and cloud-processing pathways reported in previous studies, while acknowledging that our measurements do not directly constrain the occurrence or relative importance of these processes.

The interpretation is supported by the dominance of highly oxygenated dicarboxylic acids, the highly aged character of the aerosol, and previous observations of cloud-processed aerosol characteristics at this site. However, we now explicitly acknowledge that these observations provide only indirect evidence and do not uniquely demonstrate aqueous-phase processing during transport. Accordingly, we have revised the wording throughout the manuscript and present aqueous/cloud processing as a plausible explanation, supported by the molecular composition, rather than as a directly observed mechanism.

**Changes to the manuscript**

In section 3.5:

Oxalic acid is the most abundant organic acid in tropospheric aerosol particles. Although it can be directly emitted from biomass burning and fossil fuel combustion, these sources are minor in comparison to its production via aqueous processing and photochemistry (Ervens et al., 2011; Hilario et al., 2021). Oxalic acid has been demonstrated to be the most prominent product of cloud processing (Sorooshian et al., 2006). Consequently, its status as one of the most abundant organic compounds observed at MCOH is consistent with prolonged atmospheric ageing and aqueous or cloud processing during transport from the South Asian continent. This interpretation is further supported by the concurrent abundance of other dicarboxylic acids and organic acids, together with the highly oxidised bulk organic aerosol observed by the AMS (O:C = 1.04, and high $f_{44}$), all of which indicate extensive photochemical and multiphase oxidation. The importance of aqueous processing is also evident in previously published aerosol number size distribution data from the site, which show a bimodal distribution (Budhavant et al., 2018) characteristic of aerosol populations that have undergone chemical cloud processing (Feingold and Kreidenweis, 2000; Hoppel et al., 1994).

And:

Together, observations indicate a photochemically aged air mass that has been influenced by both anthropogenic and biogenic sources. However, the measurements presented here do not directly constrain these processes; therefore, this interpretation should be regarded as a plausible explanation based on molecular composition and prior literature, rather than a direct process-level observation.

4. **If the authors intend to argue that the observed aerosol was influenced by aged outflow from Delhi or the Indo-Gangetic Plain, a more explicit period classification would be needed. In particular, the manuscript should identify the periods most strongly affected by air masses passing over Delhi-related source regions, and examine whether these periods exhibit distinguishable chemical signatures, such as source tracers, oxidation characteristics, or specific molecular patterns. Without such stage-resolved analysis, the comparison with Delhi remains suggestive rather than demonstrating that the observed aerosol characteristics at MCOH are specifically linked to aged Delhi outflow.**

We thank the reviewer for this important observation. We agree that the data do not allow us to demonstrate Delhi-specific influence. We have therefore revised the manuscript to frame Delhi as an

illustrative continental source region and interpret the MCOH aerosol as aged regional South Asian outflow.

In addition, we have deepened our analysis of the chemical characteristics of aerosol to provide more insight into source regions and formation processes. As well as the analysis discussed above, which identified a higher relative abundance of sulfate as an indication of aerosol origin in the IGP, we have carried out positive matrix factorisation (PMF) on the AMS dataset, and we have expanded the analysis of SCOs, including an analysis of thermogram shapes, species correlations, and back trajectories.

The PMF showed that the dominant aerosol factor was low-volatility oxidized organic aerosol (LV-OOA), indicative of an aged aerosol mass. The analysis identified two LV-OOA factors, one of which aligned more closely with sulfate concentrations and therefore may be more indicative of aerosol directly influenced by IGP pollution. One semi-volatile oxidised organic aerosol (SV-OOA) factor was observed, which is likely indicative of younger aerosol. The fourth factor was a mixture of hydrocarbon-like organic aerosol (HOA) and biomass burning organic aerosol (BBOA). This contributed considerably less mass than the other three and is almost certainly indicative of local sources.

The deeper analysis of SCO species indicated that the overall abundance of SCOs was more closely correlated with the signal of H2O4S I- than with sulfate, suggesting that the limiting factor in the formation of SCOs in this region is likely aerosol acidity rather than sulfate availability.

**Changes to the manuscript**

Details of text and figures added to the manuscript to support the PMF analysis and the further analysis of SCO species can be found in the response to reviewer 2.

In addition:

Section 3.6, current: "…which is used as an illustrative example of the chemical composition in the source region. This provides some insight into the impact of processing and transport on aerosol chemical characteristics."

New: …which is used as an illustrative example of aerosol composition in a highly-polluted continental environment within South Asia. The purpose of this comparison is not to demonstrate a direct influence of Delhi emissions on aerosol observed at MCOH, but rather to provide insight into the compositional differences between a continental source region and the aged aerosol observed after regional transport over the northern Indian Ocean.

**Specific comments:**

1. **The resolution of figures should be improved.**

Figures with low resolution have been replaced with higher-resolution versions in the updated manuscript.

2. **Figure 2: The colors used for the chemical species in panel (a) should be consistent with those used in panel (c) for clarity and easier comparison.**

The red bars in Fig. 2a were patterned to improve readability for red-green colourblind individuals, while maintaining adherence to the RGB values typically used to represent AMS data. However, we agree with the reviewer that the dense white pattern changes the apparent colour of the bars in the figure, which is confusing. We have changed the pattern used to address this issue.

3. **Line 273-274: Please provide more details regarding the anthropogenic sources referred to here.**

Updated text: Previous studies have found that the majority of non-sea-salt sulfate at MCOH is inorganic and originates from anthropogenic sources: the largest of these is coal-fired power plants, with other sources including brick kilns, waste burning and biomass burning. These sources release $SO_2$, which oxidises to particulate sulfate (Budhavant et al., 2024; Chutia et al., 2022; Clarke et al., 2026; Jain et al., 2019; Spencer et al., 2008).

4. **Line 275-276: Please clarify what additional information Figure S4 provides and how it supports the discussion in this section.**

This figure indicates that the calibration of the CIMS for sulfate is not perfect, as shown by the divergence between the AMS and CIMS observations of sulfate at some times, but the overall shape and magnitude are similar enough that we are confident in exploring the CIMS data in more detail.

We have updated the text to reflect this: The measurements do not track one another perfectly, but the general shape is similar and the magnitudes are comparable. This indicates that the CIMS results are conveying a meaningful signal.

5. **Line 304: Since C4H9O4S was identified during this campaign, it would be valuable to further examine its temporal evolution, diurnal pattern, and variations across the different periods. Such analyses could provide useful insight into its potential formation pathways.**

We have now looked more closely at this compound's characteristics, including its temporal pattern, correlations with other species, back-trajectory analysis, and thermogram analysis. This compound correlates closely with the presence of sulfate, and a concentration-weighted back trajectory analysis indicates that it is observed most strongly in air masses originating from the IGP. This contrasts with the majority of other observed SCOs, which correlate more closely with $H_2O_4S\ I^-$ than sulfate.

This compound was not observed in a previous campaign that observed SCOs at MCOH using Ultra-Performance Liquid Chromatography (UPLC), but it dominated the SCO signal here. This suggests the possibility that it may represent an artefact of the FIGAERO-CIMS desorption process – either as a thermal decomposition product of a larger parent ion, or evidence of sulfate-initiated chemistry taking place during the desorption process – rather than representing a compound that genuinely dominates the ambient SCO population in this region.

Nevertheless, the greater abundance of this compound in air masses that are most strongly influenced by the IGP indicates that its presence, whether from ambient detection or as an artefact formed from the presence of other species during desorption, does give a strong indication of air mass transport history.

We have updated the manuscript to reflect this.

**Changes to the manuscript:**

In section 3.4: The largest SCO signal by a large margin was $C_4H_9O_4S^-$, observed at *m/z* 153, which was also observed clustered with the iodide reagent ion as $C_4H_{10}O_4S\ I^-$ at *m/z* 281. The molecular formula is consistent with diethyl sulfate, which may plausibly form through reactions involving sulfuric acid and alcohol precursors (Japar et al., 1990). However, the molecular formula alone cannot uniquely determine the molecular structure, and alternative isomers cannot be excluded. To our knowledge, this molecular formula has not previously been reported as a dominant SCO in ambient aerosol, and it was not observed during a previous field campaign at this site (Stone et al., 2012) . Given this, it

cannot be excluded that this signal may represent an artefact introduced during the FIGAERO-CIMS analysis process: either from the thermal decomposition of a larger, parent molecule (Buchholz et al., 2020; Stark et al., 2017), or as the result of clustering or chemical reactions occurring on the heated filter during desorption or within the CIMS ion-molecule reactor. The formula $C_4H_{10}O_7S_2\ I^-$, which is consistent with $C_4H_{10}O_4S\ I^-$ clustered with $SO_3^-$, was also observed. However, it is difficult to identify whether one of these is present in ambient air and reacts to form the other, or whether both are artefacts of a third process. The signal strength for this formula shows a relatively strong correlation with AMS observations of $SO_4^{2-}$ (R = 0.61), and concentration-weighted back trajectories indicate that the air masses in which the signal was strongest originated in the Indo-Gangetic Plain (Fig. S9a). Thus, despite some ambiguity in the process leading to the observed formula, it does appear to be a genuine tracer for sulfate chemistry in the largely anthropogenic plume originating from the Indo-Gangetic Plain.

We have also added a concentration-weighted back trajectory for $C_4H_{10}O_4S\ I^-$ to the supplement, which demonstrates its association with aerosol originating from the IGP, and we have updated the conclusion to acknowledge the probability that this compound may be a measurement artefact.

6. **Sections 3.5: More in-depth analysis of the identified organic compounds is needed. For example, what is the mass fraction of each major species, and what are their temporal patterns? In addition, is the high contribution of organic acids and dicarboxylic acids distinct from that observed in other regions? In its current form, this section is largely descriptive and mainly reports several phenomena, but a deeper investigation of the organic molecular composition would substantially strengthen the manuscript.**

We thank the reviewer for this suggestion, and we agree that a more comprehensive interpretation of the molecular composition will strengthen the manuscript. Accordingly, we have substantially revised section 3.5. Specifically, we have now added a column in Table 3 (previously table 2) indicating the percentage contribution of each compound to the total organic aerosol signal.

The revised text now emphasises that the identified compounds account for approximately 49% of the detected CHO signal, with dicarboxylic acids contributing around 22%. We further discuss how the predominance of low molecular weight organic acids, together with the high O:C ratio, elevated f44, and the dominance of oxygenated organic aerosol, consistently indicates extensive atmospheric ageing due to long-range transport. We have included further analysis of how these observations compare with the literature.

Given the shorter time series available from the FIGAERO-CIMS during this campaign (10 days vs 36 days for the AMS), a robust temporal characterisation of organic molecules observed by this instrument was not possible. However, the addition of the PMF results from the AMS in the new Section 3.6 now supports the discussion in Section 3.5 by adding a temporal dimension.

**Changes to the manuscript**

- A new column has been added to Table 3 (previously Table 2) indicating the percentage contribution to the CHO signal for each identified compound.

Section 3.5 has been re-written:

The particle-phase organic aerosol at MCOH was dominated by highly oxygenated, low-molecular-weight compounds, which indicates extensive atmospheric processing prior to arrival at the receptor site. A list of 19 identified organic molecular formulae, which make up 49% of the total CHO signal, is provided in Table 3, together with potential compound names and sources. Of the total peak-fitted

CHO compounds, 22% of the signal by mass was made up of dicarboxylic acids, which are common components of organic aerosol. The most abundant individual formulae were compatible with assignment as fumaric/maleic acid (4.8%), glycolic acid (4.8%) and oxalic acid (4.7%). Collectively, the prevalence of these low-molecular-weight, more oxygenated compounds indicates that secondary formation processes substantially outweigh direct primary emissions in determining the molecular composition of organic aerosol over the northern Indian Ocean.

Oxalic acid is the most abundant organic acid in tropospheric aerosol particles. Although it can be directly emitted from biomass burning and fossil fuel combustion, these sources are minor in comparison to its production via aqueous processing and photochemistry (Ervens et al., 2011; Hilario et al., 2021). Oxalic acid has been demonstrated to be the most prominent product of cloud processing (Sorooshian et al., 2006). Consequently, its status as one of the most abundant organic compounds observed at MCOH is consistent with prolonged atmospheric ageing and aqueous or cloud processing during transport from the South Asian continent. This interpretation is further supported by the concurrent abundance of other dicarboxylic acids and organic acids, together with the highly oxidised bulk organic aerosol observed by the AMS (O:C = 1.04, and high $f_{44}$), all of which indicate extensive photochemical and multiphase oxidation. The importance of aqueous processing is also evident in previously published aerosol number size distribution data from the site, which show a bimodal distribution (Budhavant et al., 2018) characteristic of aerosol populations that have undergone chemical cloud processing (Feingold and Kreidenweis, 2000; Hoppel et al., 1994).

The ratio of malonic acid (C3) to succinic acid (C4) has been used in the literature as a proxy to assess the extent of photochemical ageing. Fresh emissions from fossil fuels and other combustion sources typically have a low C3:C4 ratio (0.25–0.44), while aged marine aerosols with a biogenic origin have higher ratios (between 1 and 11) (Bikkina et al., 2015; Kawamura and Bikkina, 2016). Here, C3:C4 was 1.69 (std = 0.35), which is consistent with photochemically aged aerosol.

Glycolic acid similarly indicates a more aged aerosol mass; it has previously been identified in marine aerosol and associated specifically with a marine microbial origin (Miyazaki et al., 2014). Fumaric/maleic acid, in contrast, is more likely to be associated with the ageing of VOCs with an anthropogenic origin (Röhrl and Lammel, 2002; Sato et al., 2021).

None of the compounds listed in Table 3 demonstrated a strong diel pattern. Rather, the ratios between them remained relatively steady, and varied most strongly with the overall concentration of organic aerosol. Together, observations indicate a photochemically aged air mass that has been influenced by both anthropogenic and biogenic sources. However, the measurements presented here do not directly constrain these processes; therefore, this interpretation should be regarded as a plausible explanation based on molecular composition and prior literature, rather than a direct process-level observation.

The molecular composition observed at MCOH differs from that typically reported in urban, or downwind of urban, regions across South Asia, where primary sources – including fresh biomass burning, traffic, industrial and cooking-related emissions – generally dominate, and nitrogen-containing organic aerosol is more abundant (eg Boreddy et al., 2021; Fu et al., 2010; Kumar et al., 2022). Instead, the dominance of small dicarboxylic acids and multifunctional organic acids at MCOH reflects extensive oxidation during transport and is consistent with previous observations of aged continental outflow reaching remote marine environments (Bikkina et al., 2023, 2015). These observations provide consistent evidence that the organic aerosol reaching MCOH is a chemically mature, regionally mixed population dominated by secondary processing.

Responses to Reviewer 2

**This study utilizes advanced HR-ToF-AMS and FIGAERO-CIMS to conduct a detailed characterization of the chemical composition of wintertime, anthropogenic-influenced haze aerosols over the northern Indian Ocean. Obtaining such high-time-resolution and molecular-level joint observational data in this relatively under-sampled region is highly valuable. The dataset contributes positively to our understanding of the evolution of long-range transported aerosols in South Asia. However, despite the exceptional richness and potential of the acquired dataset, the current analysis primarily remains at the level of species identification and bulk composition description. It does not yet fully utilize the quantitative and source apportionment capabilities of both AMS and FIGAERO-CIMS datasets. I suggest that the authors further deepen their data analysis to more robustly substantiate the core conclusion that aerosol aging during long-range transport governs the chemical composition over the northern Indian Ocean.**

We thank the reviewer for this overview, and agree that a deeper analysis could improve our understanding of the results from this campaign. We have explored further analyses based on the reviewer's suggestions, and have made substantial revision to the manuscript to reflect this. Specific points raised by the reviewer have been answered in more detail below.

**Major Comments:**

**While this study employs top-tier mass spectrometry techniques, the current analysis of OA properties remains largely at the level of bulk classification and qualitative molecular identification. It is highly recommended that the authors perform Positive Matrix Factorization (PMF) on both the AMS organic mass spectra and the FIGAERO-CIMS datasets. For the AMS, PMF would quantitatively deconvolve the contributions of secondary organic aerosols with varying degrees of oxidation (e.g., OOA) and primary emissions (e.g., BBOA, HOA). For the FIGAERO-CIMS, PMF would help categorize hundreds of complex organics into meaningful factors sharing common volatility or source characteristics. Including these standard yet fundamental analyses will provide richer chemical details to support the narrative of aerosol aging during long-range transport.**

We thank the reviewer for this valuable suggestion. On the reviewer's recommendation, we have now carried out PMF analysis for the high-resolution AMS results. A three-factor solution has been identified, which consists of a low-volatility oxygenated organic aerosol (LV-OOA) factor, a semi-volatile oxidised organic aerosol (SV-OOA) factor and a primary aerosol factor that includes a mixture of hydrocarbon-like organic aerosol (HOA) and biomass burning organic aerosol (BBOA).

The LV-OOA factor accounts for 58% of the organic aerosol mass and is dominated by oxygenated species, primarily the $CO_2$ fragment at *m/z* 44, which indicates a highly aged aerosol. The HOA/BBOA factor contributes only 5% to the overal organic aerosol mass. These results provide quantitative support for our conclusion that aerosol over MCOH is strongly influenced by long-range atmospheric processing.

We have also explored PMF analysis of data from the FIGAERO-CIMS. However, given the short timeframe during which the CIMS was operational (approximately 10 days), the solutions were unstable and difficult to distinguish from noise. Instead, we have expanded analysis of the temporal and diel behaviour of specific compounds. Details about this analysis are expanded on further down in this document, in our response to questions below.

**Changes to the manuscript:**

The results from the PMF analysis have been added to the supplement (Fig. S11), as have figures showing the results of concentration-weighted back trajectory analysis (Fig. S12). The following text has been added to the manuscript:

**3.6 Source apportionment of organic aerosol using Positive Matrix Factorisation**

Positive matrix factorisation (PMF; Ulbrich et al., 2009) was applied to the high-resolution AMS organic mass spectra to investigate the sources and degree of processing of organic aerosol observed at MCOH. This approach is commonly employed with AMS data to break down the observed mass spectrum into non-negative factor contributions representing different sources or chemical signatures, and has been described in detail elsewhere (Crippa et al., 2013). A four-factor solution was required before a clear hydrocarbon-like organic aerosol (HOA) signal emerged. However, the mass spectra for two of the remaining factors were similar, and a slight anti-correlation in signal strength throughout the time series (with one factor increasing as the other decreased, without a clear physical interpretation), indicated that this may represent the artificial "splitting" of a single low-volatility oxygenated organic aerosol component (Ulbrich et al., 2009), rather than two genuinely distinct factors. These have therefore been combined into a single LV-OOA factor, to give a final three-factor solution.

The three identified factors consisted of one mixed hydrocarbon-like organic aerosol and biomass burning organic aerosol (HOA/BBOA) factor, one semi-volatile oxygenated organic aerosol (SV-OOA) factor, and the LV-OOA factor discussed above (See Fig. S11).

The HOA/BBOA factor accounted for approximately 5% of the total organic aerosol mass. It was characterised by large peaks at *m/z* 55 ($C_4H_7$) and *m/z* 57 ($C_4H_9$), both of which are typically associated with traffic exhaust (Canagaratna et al., 2004), and a small signal at *m/z* 60 ($C_2H_4O_2$), which is typically identified as a fragment of levoglucosan or other anhydrous sugars, and considered a tracer for fresh biomass burning (Alfarra et al., 2007; Schneider et al., 2006). It shows a slight decrease in concentration during the day, which can be attributed to a combination of variability in sources – with biomass burning for cooking, for example, being more likely to occur in the evenings – and changes in boundary layer height allowing more dilution during daylight hours. Concentration-weighted back trajectory analysis indicated that there was no clear preference in source region for this factor (Fig. S12).

The LV-OOA factor accounted for approximately 58% of organic aerosol mass. It was dominated by oxygenated fragments, with CHO compounds making up 69% of the organic aerosol mass. There was variation in this factor's concentration over the period of the campaign, but it did not show a diel pattern, which is consistent with the expected behaviour of long-range transported aerosol. A concentration-weighted back trajectory analysis demonstrated that there was no preferential source region for this factor (Fig. S12).

The SV-OOA factor contributed approximately 36% of the organic aerosol mass and, while still dominated by more oxygenated aerosol, it has a higher contribution from hydrocarbon (CH) fragments than the LV-OOA factor. This factor exhibited a slight increase during the evening and night, which is characteristic of semi-volatile aerosol and suggests more local formation than for the LV-OOA factor. Organic markers that have previously been identified with marine organic aerosol, such as $CH_3SO_2$ (*m/z* 79) (Crippa et al., 2013), were not observed in high concentrations in this factor, nor in the HOA/BBOA or LV-OOA factors, which suggests that the influence of secondary aerosol formation from marine sources such as methanesulfonic acid (MSA) is not a dominant source of aerosol in this region. This finding is consistent with the low concentrations of dimethyl sulfide (DMS) observed at MCOH.

Concentration-weighted back trajectory analysis demonstrated a slightly higher concentration for this factor when the sampled air mass originated from the north. This indicates that it may be associated with the oxidation of VOC emissions from islands north of Hanimaadhoo, or of VOCs emitted from the ocean surface layer. A similar signature – with a very slight evening/night-time increase and a slight increase in abundance in northerly air masses – was not clearly observed among any compounds identified using the CIMS. However, this is likely a result of the shorter time-series available for CIMS data during this campaign (10 days, in comparison with 36 days of available AMS data). In a longer campaign, it is likely that a similar signal would be discernible in both instruments.

Overall, the dominance of high-oxygenated factors quantitatively supports the conclusion that organic aerosol reaching MCOH is highly processed during long-range transport.

**The identification of multiple SCO and CHO/CHON compounds is a noteworthy contribution of this study. However, the current analysis relies primarily on species listing and relative signal comparisons. We suggest the authors go further by quantifying the contributions of these compounds — or their compound classes — to total OA (e.g., as relative abundances or semi-quantitative mass fractions), and by examining their temporal co-variation with sulfate, relative humidity, fire counts, and air mass origin. Where secondary formation pathways are proposed for specific SCOs, supporting the discussion with relevant tracer correlations or diagnostic ratios would better constrain the inferred mechanisms. For newly identified species in particular, supplementary evidence such as characteristic thermogram profiles or comparisons with volatility data reported in the literature would strengthen confidence in the proposed assignments.**

On the reviewer's recommendation, we have expanded our analysis to quantify the relative contribution of each identified compound to its compound class, and we have investigated the temporal behaviour of selected compounds in more depth, as well as investigating the thermograms for SCO compounds.

**Changes to the manuscript:**

- An extra column has been added to Table 3 (previously Table 2), providing each identified compound's percentage contribution to total organic aerosol signal. This has *not* been added for the SCOs in Table 2 (previously Table 1): for compounds that were not ionised via the iodide adduct, it is not clear that the ionisation process would be consistent enough across all compounds to give a true measure of atmospheric abundance. We are therefore concerned that including these values would be misleading.
- We have included a more detailed discussion of the various SCO compounds identified in Table 1, including back trajectory analysis, discussion of correlations with one another and with $SO_4^{2-}$, and conclusions that can be inferred about sources and formation pathways. We have supported this discussion with the following figures, added to the supplement:
    - Fig. S10: A correlation matrix for the identified SCOs.
    - Fig. S9: A plot showing the concentration-weighted back trajectories for a selection of SCOs.

Added to the manuscript:

Of the identified SCOs listed in Table 2, the majority are short-chain and highly-oxidised. The oxygen-to-carbon (O:C) ratios vary between 1 and 2, and 50% of the identified compounds contain four carbon atoms (C4), with the remainder having between 2 and 5 (C2–C5). Several of the observed compounds have previously been identified as oxidation products of isoprene in the presence of sulfate particles (Le Breton et al., 2018; Wang et al., 2021; Zhu et al., 2025). There were strong correlations between

many of the C4 and C5 compounds, indicating a similar formation process (Fig. S10). A concentration-weighted back trajectory analysis was carried out for the sum of the signals of the eight most strongly correlated SCOs (0.62 <= R <= 0.89; Fig. S9b). The result indicated that there was no clear preferential source region for these compounds. There was no strong relationship, on average, between the concentration of $SO_4^{2-}$ observed by the AMS and the SCOs in Table 2 (average R = 0.10, standard deviation = 0.22), but there was evidence of a stronger relationship with $H_2SO_4$ $I^-$, observed by the CIMS (average R = 0.48, standard deviation = 0.17). This association may reflect differences in sulfate speciation or FIGAERO desorption chemistry; because $H_2SO_4$ $I^-$ is also produced from ammonium sulfate during calibration, it should not be interpreted as a direct quantitative measure of aerosol acidity.

And

Glycolic acid sulfate (GAS) was observed during this campaign, and has been identified as a product of aqueous photochemistry after glyoxal has been taken up by sulfate-containing aerosol (Galloway et al., 2009). Several of the larger SCO signals observed were small chain (C2, C3) acids, which could potentially follow a similar formation pathway to GAS, forming as a result of aqueous photochemistry. Similar to the larger C4 and C5 compounds, concentration-weighted back trajectory analysis did not indicate a preferential source region for these compounds.

- We have included an analysis of the thermograms for the SCOs identified in Table. 1, including grouping these by characteristic shapes and discussing the implications of these. We have supported this discussion with the new Fig. 6, which shows the average thermogram across the campaign for each of these compounds. Newly identified compounds are highlighted in this figure, to aid the comparison with other compounds.

Added to the text:

Thermograms, which were produced as the filter in the FIGAERO is heated to 200 °C over the course of 20 minutes, provide some information about compound volatility and morphology. The mean normalised thermograms for all compounds identified in Table 2 have been plotted in Fig. 6. Here, it can be seen that the shape of these thermograms fall roughly into three groups. In the first group, the thermograms are an almost identical shape after normalisation, with a clear maximum temperature ($t_{max}$) at around 146 °C. This shape almost perfectly follows the thermogram shape shared by several inorganic sulfate peaks, including $H_2O_4S$ $I^-$, $O_3S^-$ and $HO_4S^-$. In group 2, thermograms appear to follow this same basic shape as group 1, with the same $t_{max}$, but with a broader peak, and with many displaying a shoulder or even a second, lower peak at lower temperatures. For group 3 compounds, the $t_{max}$ is much lower – between 105 °C ($C_4H_9O_7S^-$) and 128 °C ($C_5H_7O_7S^-$) – but the signal increases into a second peak again at higher temperatures – in most cases above 160 °C.

The high desorption temperatures for SCOs is consistent with previous literature suggesting that organosulfates have low volatilities (Brüggemann et al., 2020). The identical shape shared by all group 1 compounds, as well as the larger peak in the group 2 thermograms and a number of inorganic sulfate species, may indicate that these compounds share similar thermal properties and volatilities. However, given the high $t_{max}$ and the small size of some of these compounds (for example, $C_2H_3O_5S^-$ and $C_2H_3O_6S^-$), this is surprising. A second interpretation could be that some of these are formed as thermal decomposition products of a larger parent molecule (Buchholz et al., 2020; Schobesberger et al., 2018), or that further sulfate chemistry may have taken place during the desorption process, leading to several products with identical desorption patterns.

Thermograms with several peaks, as is seen in groups 2 and 3, can indicate either the presence of different isomers with different volatilities, or the influence of different processes during desorption (Buchholz et al., 2020; Schobesberger et al., 2018). In the case of group 3, the high temperature of the second desorption peak suggests that this peak may be associated with the thermal decomposition of a larger, less volatile parent molecule. The $t_{max}$ observed at lower temperatures, in contrast, likely represents the desorption of the genuine parent molecule present in ambient air.

- We have extended the concluding paragraph of the SCO section, to take these alterations into account.

Added to the manuscript:

Taken together, these observations indicate the strong influence of both acid-catalysed epoxide reactions and aqueous phase chemistry in driving the formation of SCOs in this region. It is likely that species identified in the CIMS dataset represent a combination of genuine parent molecules present in ambient air, and of thermal decomposition products of larger parent species or products of further chemical reactions during desorption. However, these results unambiguously highlight the importance of sulfate chemistry, and interactions between biogenic/anthropogenic VOCs and sulfate aerosol, in the aerosol plume.

**The text highlights $C_4H_9O_4S^-$ as the most abundant SCO signal observed, proposing it corresponds to diethyl sulfate and claiming this as its first ambient atmospheric detection. Currently, however, the assignment relies primarily on molecular formula matching, lacking further validation such as comparisons with standard thermograms, literature values of known organosulfate volatilities, or a discussion ruling out potential isomers. Given that this is a key highlight of the paper, it is recommended that the authors explicitly acknowledge the uncertainties associated with this identification and provide as much corroborative analysis as possible, allowing readers to objectively assess the robustness of this claim.**

We thank the reviewer for this important comment, and agree that the molecular formula alone cannot uniquely determine the structure, nor is it a guarantee that this formula represents the parent compound as it is present in ambient air. We have therefore revised the manuscript to emphasise that the assignment is tentative. In addition, we have examined the characteristics of this signal more closely. Given the dominance of this signal in our dataset, despite the fact that it has not been observed previously, it is plausible that this is formed as an artefact during the desorption process, either as a fragment from a larger parent compound, or as a result of sulfate chemistry occurring during the desorption process. We have updated the manuscript to acknowledge this possibility.

The presence of this compound does appear to correlate with the presence of $SO_4^{2-}$ in the aerosol, and a concentration-weighted back trajectory analysis indicates that it is observed most strongly in air masses originating from the Indo-Gangetic Plain (IGP). This suggests that, despite the uncertainty in its formation mechanism, this compound or artefact likely can be considered a tracer for sulfate aerosol originating from the IGP. This contrasts with other observed SCOs in this dataset, which do not correlate as closely with sulfate and which do not preferentially appear in aerosol originating from the IGP.

We have re-visited the peak fitting to evaluate our confidence in the assignment of this molecular formula. For $C_4H_9O_4S^-$, the assigned formula was at 4.58 ppm from the fitted peak maximum, and for $C_4H_{10}O_4S\ I^-$, it was at 7.21 ppm. In both cases, there was no other plausible peak identification within 20 ppm. We are therefore confident in the assignment of this formula.

**Changes to the manuscript:**

The largest SCO signal by a large margin was $C_4H_9O_4S^-$, observed at *m/z* 153, which was also observed clustered with the iodide reagent ion as $C_4H_{10}O_4S\ I^-$ at *m/z* 281. The molecular formula is consistent with diethyl sulfate, which may plausibly form through reactions involving sulfuric acid and alcohol precursors (Japar et al., 1990). However, the molecular formula alone cannot uniquely determine the molecular structure, and alternative isomers cannot be excluded. To our knowledge, this molecular formula has not previously been reported as a dominant SCO in ambient aerosol, and it was not observed during a previous field campaign at this site (Stone et al., 2012) . Given this, it cannot be excluded that this signal may represent an artefact introduced during the FIGAERO-CIMS analysis process: either from the thermal decomposition of a larger, parent molecule (Buchholz et al., 2020; Stark et al., 2017), or as the result of clustering or chemical reactions occurring on the heated filter during desorption or within the CIMS ion-molecule reactor. The formula $C_4H_{10}O_7S_2\ I^-$, which is consistent with $C_4H_{10}O_4S\ I^-$ clustered with $SO_3^-$, was also observed. However, it is difficult to identify whether one of these is present in ambient air and reacts to form the other, or whether both are artefacts of a third process. The signal strength for this formula shows a relatively strong correlation with AMS observations of $SO_4^{2-}$ (R = 0.61), and concentration-weighted back trajectories indicate that the air masses in which the signal was strongest originated in the Indo-Gangetic Plain (Fig. S9a). Thus, despite some ambiguity in the process leading to the observed formula, it does appear to be a genuine tracer for sulfate chemistry in the largely anthropogenic plume originating from the Indo-Gangetic Plain.

We have also added the following figure to the supplement:

- Fig. S9b: The concentration-weighted back trajectory for $C_4H_{10}O_4S\ I^-$, which demonstrates its origin in the IGP.

**Minor Comments:**

**The study selects three characteristic sampling periods based on 10-day backward trajectories to compare mass spectra and aerosol composition. It is recommended to supplement this with statistical significance testing (e.g., t-tests on the mass fractions of major components) across these periods. This would provide a more objective evaluation of whether the chemical composition features associated with different source regions are statistically distinct.**

We thank the reviewer for this suggestion, and agree that the comparison across these three periods as it was presented was not statistically robust.

However, the nature of the time series data presented here makes it challenging to perform statistical tests such as a t-test. These tests only produce a robust result in cases where samples are independent, normally distributed, and sufficient in number.

Time series data suffers from autocorrelation – where one data point is likely to be similar to the previous, and so cannot be considered truly independent – which leads them to over-state significance. We have carried out a Durbin-Watson test to identify the influence of autocorrelation within our dataset, using the organic aerosol time series as an example (see the figure to the left). For the raw data (time step = 30 s), the d-statistic was 0.038, where values close to 0 indicate strong autocorrelation, and values near 2 indicate no autocorrelation. We averaged the data to increasingly large time bins and found that the influence of auto-correlation was only statistically significantly absent when the averaging time was 39 hours or greater. However, given the duration of the selected time periods (four days), averaging these datasets to reduce the influence of autocorrelation would not provide enough individual data points to carry out robust statistical tests.

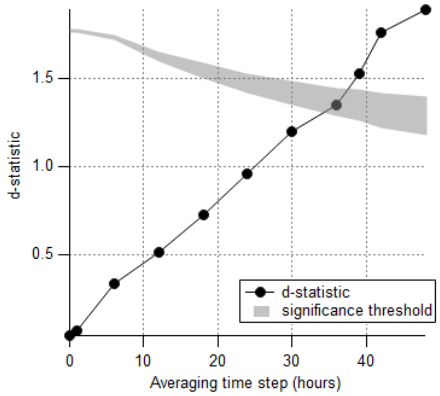


However, we agree that a deeper comparison is required here. We have therefore now included more information about the chemical characteristics of aerosol observed during these time periods, both in the text and summarised in a new table, Table 1. While this is not as statistically conclusive as a t-test may have been, we believe it provides sufficient evidence to explore the difference between the time periods.

Furthermore, we have added more nuance to our original interpretation that there was very little chemical difference between the three periods. We note, now, that the ratio between $SO_4^{2-}$ and organic aerosol does, in fact, vary throughout the campaign, increasing from one period to the next. We have carried out a concentration-weighted back trajectory, which suggests that sulfate is more prominent in aerosol originating from the IGP. We have also included further chemical information to support our original interpretation that the characteristics of the organic aerosol are remarkably similar regardless of the air mass transport history.

**Changes to the manuscript**

In section 3.2:

The comparison of the three transport periods indicates that, although sulfate remained the dominant species in all cases, the fractional contribution of sulfate increased from one period to the next, while that of organic aerosol decreased. The contribution from nitrate remained low throughout. The chemical composition of organic aerosol was highly consistent across all three time periods. Characteristic parameters from all three time periods are shown in Table 1. Here it can be seen that the O:C ratio, H:C ratio, and the fractional contribution from *m/z* 44 ($f_{44}$), *m/z* 43 ($f_{43}$) and *m/z* 60 ($f_{60}$) showed very little variation, regardless of air mass origin. This compositional stability in organic aerosol across air masses arriving from different transport pathways suggests that the aerosol reaching MCOH had undergone extensive regional mixing and atmospheric processing before arrival. Consequently, differences in transport history were reflected more strongly in aerosol loading than in aerosol composition, indicating that regional-scale processing exerts a dominant influence on the chemical characteristics of the wintertime haze over the northern Indian Ocean.

A concentration-weighted back trajectory analysis of sulfate aerosol and organic aerosol suggests that, while both species are present in air masses regardless of transport history, the sulfate concentration is most prominent in air masses originating from the IGP, while organic aerosol did not show any preferential air mass origin (Fig. 3). This suggests that at this site, the fraction of sulfate observed in

ambient aerosol may be useful as an indication of air masses that have been more strongly influenced by anthropogenic pollution in the IGP.

Table 1: The chemical characteristics of aerosol during the three identified time periods. For O:C, H:C, f44, f43 and f60, the standard deviation (std) is shown in brackets.

| Parameter | Period 1 | Period 2 | Period 3 |
|---|---|---|---|
| Sulfate fraction (%) | 42% | 47% | 56% |
| Organic aerosol fraction (%) | 36% | 32% | 22% |
| Nitrate fraction | 2.6% | 2.1% | 1.7% |
| O:C | 1.05 (std = 0.076) | 1.03 (std = 0.052) | 1.06 (std = 0.062) |
| H:C | 1.26 (std = 0.063) | 1.21 (std = 0.040) | 1.17 (std = 0.051) |
| $f_{44}$ | 0.214 (std = 0.014) | 0.218 (std = 0.009) | 0.224 (std = 0.011) |
| $f_{43}$ | 0.038 (std = 0.006) | 0.039 (std = 0.003) | 0.037 (std = 0.004) |
| $f_{60}$ | 0.0024 (std = 0.0006) | 0.0023 (std = 0.0006) | 0.0022 (std = 0.0008) |

**The supplementary material notes that the aerosol was largely neutralized based on an ion balance analysis (indicating sufficient ammonium to neutralize sulfate and nitrate). Given that sulfate chemistry and aqueous-phase processes critically influence the formation pathways of secondary organic aerosols (especially SCOs), it is suggested to briefly discuss in the main text how this neutralized environment might specifically affect the formation mechanisms of the observed sulfur-containing organics (e.g., the efficiency of acid-catalyzed multiphase reactions).**

We agree with the reviewer that acidity is a fundamental requirement for the formation of SCOs, and that a completely neutral aerosol would therefore be unlikely to contain a large proportion of SCOs. We have expanded our discussion of SCO formation mechanisms in section 3.4, and therein noted that the concentration of SCOs appears to correlate well with observed $H_2O_4S\ I^-$. This suggests that the limiting step in the formation of SCOs in this environment is likely aerosol acidity, rather than sulfate concentration. The text added to the manuscript is shown further up, in our response to the reviewer's second comment.

## References cited in these responses


Brüggemann, M., Xu, R., Tilgner, A., Kwong, K. C., Mutzel, A., Poon, H. Y., Otto, T., Schaefer, T., Poulain, L., Chan, M. N., and Herrmann, H.: Organosulfates in Ambient Aerosol: State of Knowledge and Future Research Directions on Formation, Abundance, Fate, and Importance, Environ. Sci. Technol., 54, 3767–3782, https://doi.org/10.1021/acs.est.9b06751, 2020.

Buchholz, A., Ylisirniö, A., Huang, W., Mohr, C., Canagaratna, M., Worsnop, D. R., Schobesberger, S., and Virtanen, A.: Deconvolution of FIGAERO–CIMS thermal desorption profiles using positive matrix factorisation to identify chemical and physical processes during particle evaporation, Atmospheric Chemistry and Physics, 20, 7693–7716, https://doi.org/10.5194/acp-20-7693-2020, 2020.

Budhavant, K., Manoj, M. R., Nair, H. R. C. R., Gaita, S. M., Holmstrand, H., Salam, A., Muslim, A., Satheesh, S. K., and Gustafsson, Ö.: Changing optical properties of black carbon and brown carbon aerosols during long-range transport from the Indo-Gangetic Plain to the equatorial Indian Ocean, Atmospheric Chemistry and Physics, 24, 11911–11925, https://doi.org/10.5194/acp-24-11911-2024, 2024.

Chutia, L., Ojha, N., Girach, I., Pathak, B., Sahu, L. K., Sarangi, C., Flemming, J., da Silva, A., and Bhuyan, P. K.: Trends in sulfur dioxide over the Indian subcontinent during 2003–2019, Atmospheric Environment, 284, 119189, https://doi.org/10.1016/j.atmosenv.2022.119189, 2022.

Clarke, S., Holmstrand, H., Budhavant, K., Remani, M., Haslett, S., Rodiouchkina, K., Kooijman, E., and Gustafsson, Ö.: Isotopic apportionment of sulfate aerosols between natural and anthropogenic sources in the outflow of South Asia, EGUsphere, 1–20, https://doi.org/10.5194/egusphere-2025-5334, 2025.

Galloway, M. M., Chhabra, P. S., Chan, A. W. H., Surratt, J. D., Flagan, R. C., Seinfeld, J. H., and Keutsch, F. N.: Glyoxal uptake on ammonium sulphate seed aerosol: reaction products and reversibility of uptake under dark and irradiated conditions, Atmospheric Chemistry and Physics, 9, 3331–3345, https://doi.org/10.5194/acp-9-3331-2009, 2009.

Jain, S., Sharma, S. K., Srivastava, M. K., Chaterjee, A., Singh, R. K., Saxena, M., and Mandal, T. K.: Source Apportionment of PM10 Over Three Tropical Urban Atmospheres at Indo-Gangetic Plain of India: An Approach Using Different Receptor Models, Arch Environ Contam Toxicol, 76, 114–128, https://doi.org/10.1007/s00244-018-0572-4, 2019.

Japar, S. M., Wallington, T. J., Andino, J. M., and Ball, J. C.: Atmospheric chemistry of gaseous diethyl sulfate, Environ. Sci. Technol., 24, 894–897, https://doi.org/10.1021/es00076a017, 1990.

Le Breton, M., Wang, Y., Hallquist, Å. M., Pathak, R. K., Zheng, J., Yang, Y., Shang, D., Glasius, M., Bannan, T. J., Liu, Q., Chan, C. K., Percival, C. J., Zhu, W., Lou, S., Topping, D., Wang, Y., Yu, J., Lu, K., Guo, S., Hu, M., and Hallquist, M.: Online gas- and particle-phase measurements of organosulfates, organosulfonates and nitrooxy organosulfates in Beijing utilizing a FIGAERO ToF-CIMS, Atmospheric Chemistry and Physics, 18, 10355–10371, https://doi.org/10.5194/acp-18-10355-2018, 2018.

Schobesberger, S., D'Ambro, E. L., Lopez-Hilfiker, F. D., Mohr, C., and Thornton, J. A.: A model framework to retrieve thermodynamic and kinetic properties of organic aerosol from composition-resolved thermal desorption measurements, Atmospheric Chemistry and Physics, 18, 14757–14785, https://doi.org/10.5194/acp-18-14757-2018, 2018.

Spencer, M. T., Holecek, J. C., Corrigan, C. E., Ramanathan, V., and Prather, K. A.: Size-resolved chemical composition of aerosol particles during a monsoonal transition period over the Indian Ocean, Journal of Geophysical Research: Atmospheres, 113, https://doi.org/10.1029/2007JD008657, 2008.

Stark, H., Yatavelli, R. L. N., Thompson, S. L., Kang, H., Krechmer, J. E., Kimmel, J. R., Palm, B. B., Hu, W., Hayes, P. L., Day, D. A., Campuzano-Jost, P., Canagaratna, M. R., Jayne, J. T., Worsnop, D. R., and Jimenez, J. L.: Impact of Thermal Decomposition on Thermal Desorption Instruments: Advantage of Thermogram Analysis for Quantifying Volatility Distributions of Organic Species, Environ. Sci. Technol., 51, 8491–8500, https://doi.org/10.1021/acs.est.7b00160, 2017.

Stone, E. A., Yang, L., Yu, L. E., and Rupakheti, M.: Characterization of organosulfates in atmospheric aerosols at Four Asian locations, Atmospheric Environment, 47, 323–329, https://doi.org/10.1016/j.atmosenv.2011.10.058, 2012.

Wang, Y., Zhao, Y., Wang, Y., Yu, J.-Z., Shao, J., Liu, P., Zhu, W., Cheng, Z., Li, Z., Yan, N., and Xiao, H.: Organosulfates in atmospheric aerosols in Shanghai, China: seasonal and interannual variability, origin, and formation mechanisms, Atmospheric Chemistry and Physics, 21, 2959–2980, https://doi.org/10.5194/acp-21-2959-2021, 2021.

Zhu, Y., Li, H., Wei, J., Ding, H., Cai, D., Zou, X., Wang, G., Wang, Q., Ding, Z., Liu, Z., Chen, J., Yun, L., Deng, C., and Huang, K.: Marine Modulation of the Formation Pathways and Sources of Organosulfates over the Coastal South China Sea, Environ. Sci. Technol. Lett., 12, 739–746, https://doi.org/10.1021/acs.estlett.5c00406, 2025.